Scientia Iranica, Vol. 12, No. 4, pp 359–367

SCIENTIA
IRANICA

Simulation of Average Stress-Average Strain Relationship of Ship Unstiffened/Stiffened Plates Subject to in-Plane Compression

M.R. Khedmati[1]

In this paper, a simple and efficient analytical method, combining elastic large deflection analysis and rigid plastic mechanism analysis, is presented for derivation of the average stress-average strain relationship of plates subject to in-plane longitudinal compression. By imposing equilibrium conditions of forces and bending moments and assuming proper stress and strain distributions in the stiffened plate cross-sections, the average stress-average strain relationship of the stiffened plates is also derived. The algorithm can be easily implemented in methods for the evaluation of ship hull girder strength, as well as in the estimation of the ultimate capacity of offshore structures.

INTRODUCTION

In the design of ships and offshore structures, it is essential to ensure that the structure has sufficient strength to sustain extreme loading situations. Such marine structures are mostly assembled with plates and stiffened plates (Figure 1). The strength of such plates and stiffened plates is crucial for the overall structural capacity or, in other words, for the ultimate strength of the whole structure. For a thorough assessment of a structural design, for understanding possible improvements and for predicting the consequences in the event of failure, an approximation of the value of ultimate strength is not sufficient. The complete behavior, up to collapse and beyond, of the structure has to be simulated to gain insight into the causes and effects of a structural failure.

For the analysis of large marine structures, an accurate and efficient approach is required to obtain results within a reasonable space of time. Despite the enormous developments in computer technology, elastoplastic large deflection analyses with conventional Finite Element Analysis (FEA) are too time-consuming for large structures. Therefore, a simplified method has to be employed to reduce the computational time and/or increase the size of the structural parts that can be analyzed.

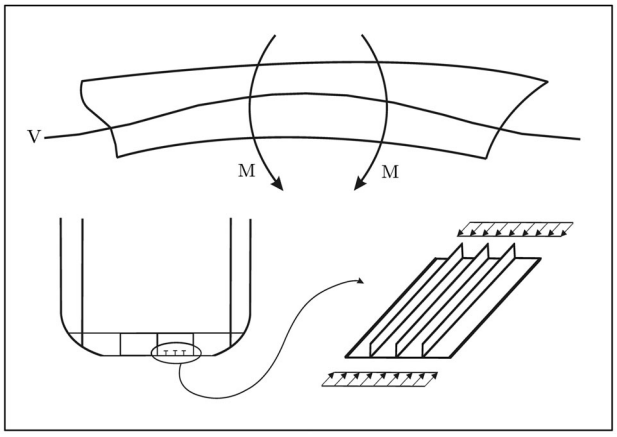

Figure 1. Ship hull girder.

Methods to obtain the moment-curvature relationship (Figure 2), considering the collapse of parts of the cross-section, have been developed for cross-sections of ships in bending. One of the best known methods is Smith's method [1,2], in which the ship cross-section is divided into small elements, each of which is composed of plates without/with stiffener. The average stress-average strain relationships of all elements are derived, before the analysis of the whole cross-section progresses, as follows: Curvature is applied incrementally about the instantaneous neutral

1. *Faculty of Marine Technology, Amirkabir University of Technology, No. 424, 15914, Tehran, I.R. Iran.*

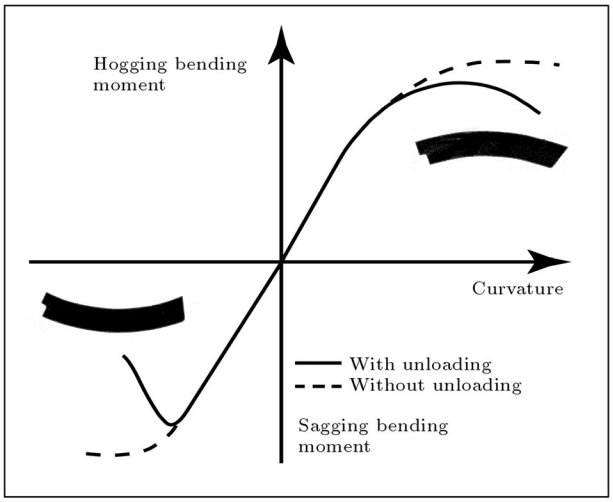

Figure 2. Typical moment-curvature relationship.

axis and the strain of each element is calculated. The corresponding stress is taken from the stress-strain curves previously derived and the corresponding moments are obtained by integration over the cross-section (Figure 3). FEA is usually applied, in order to derive the average stress-average strain relationships of plate and stiffened plate elements.

The analytical method proposed in this paper is one suitable framework for implementing a general approach to collapse analysis, since it leads to a reduction, either in time or in cost, of the solution process. Combining the theory of elastic large deflection analysis with rigid-plastic mechanism analysis, a simple formulation is expressed, in order to derive average stress-average strain relationships of plates and stiffened plates. The accuracy of the method or formulation is verified against the FEA obtained results. Employing such a formulation, the ultimate strength evaluation of ships and offshore structures is made possible in a very short time, with reasonable accuracy and cost.

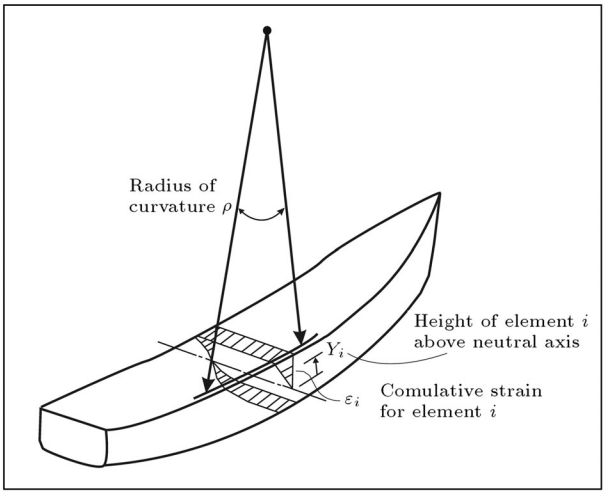

Figure 3. Ship hull girder bending concept (Smith's method).

GENERAL ASSUMPTIONS

The longitudinal stiffening system (Figure 4) is usually employed in large ships at their midlength part, especially in the deck and bottom structures. If an extreme bending moment acts on a hull girder, the highest possible collapse mode may be the overall collapse of the stiffened panels after the local collapse of individual plate elements between stiffeners. In what follows, such a collapse mode is assumed in derivation of average stress-average strain relationships of the elements.

A typical element, consisting of a stiffener with attached plating, is shown in Figure 5. This element may deflect, as indicated in Figure 5b, under axial compression. To keep the rationality of the method, the region of the element between sections 1 and 2 is considered in the modeling (double span model).

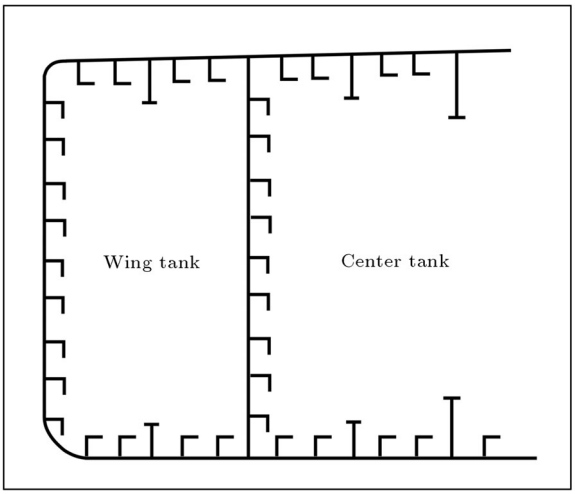

Figure 4. Longitudinal stiffening system.

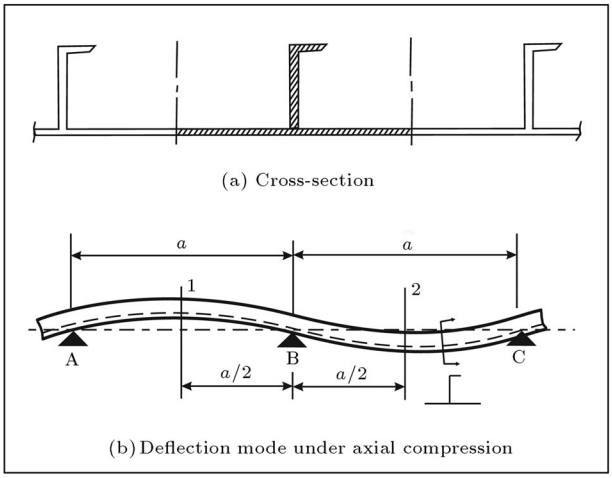

Figure 5. Stiffener (stiffened plate) element.

The following assumptions are made in the derivation of the average stress-average strain relationships of the stiffener elements:

1. Attached platings behave as isolated plates;
2. Plane cross-sections remain plane, and the strain varies linearly over the cross-section;
3. The material is assumed to be elastic-perfectly plastic;
4. The stiffener element is modeled as a continuous beam resting on simple supports;
5. The deformation in torsional buckling mode of a stiffener is not considered.

Average stress-average strain relationships of the isolated plates are derived, first, combining the results of elastic large deflection analysis and rigid plastic mechanism analysis. The average stress-average strain relationships of the stiffener elements are derived considering elastoplastic stress distributions at both ends of the element, which satisfy the equilibrium conditions of forces and moments.

AVERAGE STRESS-AVERAGE STRAIN RELATIONSHIP OF PLATES

Welding Induced Initial Deflections

The actual mode of the initial deflection of the plate is very complex. For a plate of length a, breadth b and thickness t, this complex mode can be expressed by a double sinusoidal series as:

$$w_0 = \sum_{i=1}^{\infty}\sum_{j=1}^{\infty} A_{0ij} \sin\frac{i\pi x}{a} \sin\frac{j\pi y}{b}. \tag{1}$$

When a compressive load acts in the direction of the longer side of the plate (x-direction), the deflection components in the direction of the shorter side of the plate (y-direction) decrease with the increase in load, except the first term, with one half-wave. In this case, only the first term ($j = 1$) may play a dominant role and the simpler form of initial deflection can be used for analysis as follows:

$$w_0 = \sum_{i=1}^{\infty} A_{0i} \sin\frac{i\pi x}{a} \sin\frac{\pi y}{b}. \tag{2}$$

Ueda and Yao [3] idealized this mode with another expression as follows:

$$w_0 = \sum_{i=1,3,5,\ldots}^{21} A_{0i} \sin\frac{i\pi x}{a} \sin\frac{\pi y}{b}, \tag{3}$$

which includes only odd terms. Later, Yao et al. [4] introduced even terms also in this mode and, finally, the idealized hungry-horse mode took the following form:

$$w_0 = \sum_{i=1}^{11} A_{0i} \sin\frac{i\pi x}{a} \sin\frac{\pi y}{b}. \tag{4}$$

The initial deflection is, herein, assumed to be in the idealized hungry-horse mode. The coefficients of this mode (A_{0i}), nondimensionalized by plate thickness (t), i.e., A_{0i}/t, are given in [4] as functions of the plate aspect ratio. The maximum magnitude of initial deflection, $w_{0\,\max}$, is taken as:

$$w_{0\,\max} = 0.05\beta^2 t, \tag{5}$$

where β is the slenderness parameter of the plate and defined by:

$$\beta = \frac{b}{t}\sqrt{\frac{\sigma_Y}{E}}, \tag{6}$$

in which σ_Y and E are yield stress and modulus of elasticity of the plate, respectively. The value of $w_{0\,\max}$ given by Equation 5, is the average magnitude of initial deflection of ship plates [5]. To consider the plate continuity, it is assumed that the plate is simply-supported along its four edges, which remain straight while subjected to in-plane movements.

The total deflection mode, under the action of in-plane longitudinal compression, is assumed to follow as:

$$w = \sum_{i=1}^{11} A_i \sin\frac{i\pi x}{a} \sin\frac{\pi y}{b}. \tag{7}$$

Stable Mode

According to the work presented in [4], it is shown that with an increase in the compressive load above the buckling load, just one single deflection component among the deflection components, A_i, is magnified. Consequently, taking single deflection modes, as follows, can approximate the behavior of the plate:

$$w_0 = A_{0m} \sin\frac{m\pi x}{a} \sin\frac{\pi y}{b}, \tag{8}$$

and:

$$w = A_m \sin\frac{m\pi x}{a} \sin\frac{\pi y}{b}. \tag{9}$$

In the above equations, m is the number of half-waves in the stable deflection mode above the plate buckling load and is determined as [4]:

$$m = \begin{cases} 1 : a/b < 1.3 \\ k : k - 0.7 \le a/b < k + 0.3 \end{cases}, \tag{10}$$

where a/b is the plate aspect ratio and k is an integer greater than 1. Hereafter, A_{0m} and A_m are simply denoted as A_0 and A, respectively.

Relationship Between Average Stress and Deflection

Elastic Range

The relationship between average stress and deflection in the elastic range is derived applying the Elastic Large Deflection Analysis (ELDA). The differential equation representing the compatibility condition of an initially deflected plate is expressed as:

$$\nabla^4 F = E\left[\left(\frac{\partial^2 w}{\partial x \partial y}\right)^2 - \frac{\partial^2 w}{\partial x^2}\frac{\partial^2 w}{\partial y^2} - \left(\frac{\partial^2 w_0}{\partial x \partial y}\right)^2 + \frac{\partial^2 w_0}{\partial x^2}\frac{\partial^2 w_0}{\partial y^2}\right]. \quad (11)$$

Figure 6 shows a plate under longitudinal compression, $\sigma = \sigma_x$.

Substituting the assumed initial deflection (Equation 8) and total deflection (Equation 9) into Equation 11, the Airy's stress function is obtained in the following form:

$$F = \frac{E(A^2 - A_0^2)}{32}\left[\alpha^2 \cos\frac{2m\pi x}{a} + \frac{1}{\alpha^2}\cos\frac{2\pi y}{b}\right] + \sigma, \quad (12)$$

where:

$$\alpha = \frac{a}{mb}. \quad (13)$$

Having acquired Airy's stress function, in-plane stress components are easily obtained as:

$$\sigma_{xp} = \frac{\partial^2 F}{\partial y^2}, \quad \sigma_{yp} = \frac{\partial^2 F}{\partial x^2}, \quad \sigma_{xyp} = -\frac{\partial^2 F}{\partial x \partial y}. \quad (14)$$

Applying the stress-strain relationships for the plane stress state, the corresponding in-plane strains are:

$$\varepsilon_{xp} = \frac{1}{E}(\sigma_{xp} - \nu\sigma_{yp}),$$

$$\varepsilon_{yp} = \frac{1}{E}(\sigma_{yp} - \nu\sigma_{xp}),$$

$$\gamma_{xyp} = \frac{2(1+\nu)}{E}\tau_{xyp}, \quad (15)$$

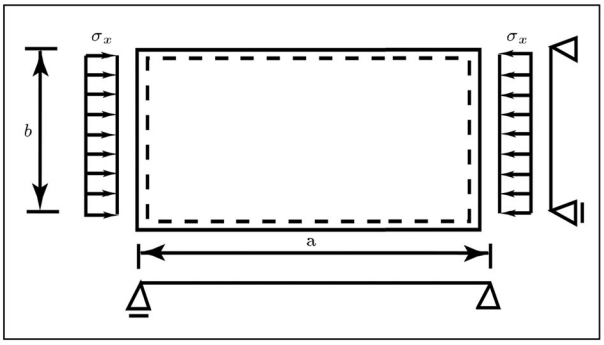

Figure 6. Rectangular plate under longitudinal compression.

where ν is Poisson's ratio. On the other hand, the bending strain components are given as:

$$\varepsilon_{xb} = -z\frac{\partial^2(w - w_0)}{\partial x^2},$$

$$\varepsilon_{yb} = -z\frac{\partial^2(w - w_0)}{\partial y^2},$$

$$\gamma_{xyb} = -2z\frac{\partial^2(w - w_0)}{\partial x \partial y}, \quad (16)$$

while the corresponding bending stress components are:

$$\sigma_{xb} = \frac{E}{1-\nu^2}(\varepsilon_{xb} + \nu\varepsilon_{yb}),$$

$$\sigma_{yb} = \frac{E}{1-\nu^2}(\varepsilon_{yb} + \nu\varepsilon_{xb}),$$

$$\tau_{xyb} = \frac{E}{2(1+\nu)}\gamma_{xyb}. \quad (17)$$

The principle of virtual work is expressed as:

$$\delta w_i = \delta w_e, \quad (18)$$

where δw_i and δw_e are the internal and external virtual work done for a virtual deflection, δA, respectively, and are expressed as:

$$\delta w_i = \int_v [(\sigma_{xp} + \sigma_{xb})(\delta\varepsilon_{xp} + \delta\varepsilon_{xb}) + (\sigma_{yp} + \sigma_{yb})(\delta\varepsilon_{yp} + \delta\varepsilon_{yb}) + (\tau_{xyp} + \tau_{xyb})(\delta\gamma_{xyp} + \delta\gamma_{xyb})]dv, \quad (19)$$

and:

$$\delta w_e = -\sigma b t \delta\overline{u}. \quad (20)$$

Therefore, the average stress-deflection relationship is obtained as follows:

$$\frac{\pi^2 E}{16b^2}\left(\frac{1}{\alpha^2} + \alpha^2\right)(A^2 - A_0^2) + \sigma_{cr0}\left(1 - \frac{A_0}{A}\right) - \sigma = 0, \quad (21)$$

where:

$$\sigma_{cr0} = \frac{\pi^2 t^2 E}{12(1-\nu^2)b^2}\left(\frac{1}{\alpha} + \alpha\right)^2, \quad (22)$$

σ_{cr0} is the buckling strength of a simply-supported rectangular plate.

Plastic Range

With the increase in the applied end-shortening displacement, a plate undergoes buckling and yielding and, then, attains its ultimate strength. After the ultimate strength, the compressive load decreases with the increase in the applied end-shortening displacement and deflection.

The average stress-plastic deflection relationship at the post-ultimate strength region, is derived according to the Rigid-Plastic Mechanism Analysis (RPMA), assuming rigid-perfectly plastic material. Depending on the plate aspect ratio (a/b), two configurations of the plastic mechanism may exist, as illustrated in Figure 7. For these mechanisms, the following relationships are derived [6]:

$$m_{45}+(1/\alpha-1)m_{90}/2=(2/\alpha-1)\overline{\sigma}.\overline{A} \quad \text{for} \quad \alpha \le 1.0, \tag{23}$$

$$m_{45}+(\alpha-1)m_0/2=\overline{\sigma}.\overline{A} \quad \text{for} \quad \alpha > 1.0, \tag{24}$$

where $\overline{\sigma}=\sigma/\sigma_Y, \overline{A}=A/t$ and:

$$m_{90}=1-\overline{\sigma}^2, \tag{25}$$

$$m_0=2m_{90}/\sqrt{1+3m_{90}}, \tag{26}$$

$$m_{45}=4m_{90}/\sqrt{1+15m_{90}}. \tag{27}$$

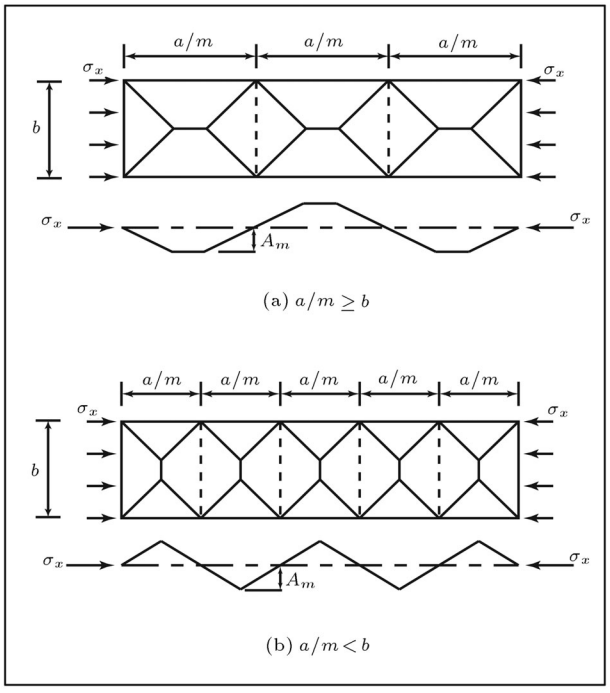

Figure 7. Plastic mechanisms of plate under compression.

Relationship Between Average Stress and Average Strain

Elastic Range

According to elastic large deflection analysis, the in-plane shortening in the x-direction will become:

$$\overline{u}=\frac{1}{b}\int_0^a\int_0^b\left[\varepsilon_x-\frac{1}{2}\left\{\left(\frac{\partial w}{\partial x}\right)^2-\left(\frac{\partial w_0}{\partial x}\right)^2\right\}\right]dydx$$

$$=-\frac{a}{E}\sigma-\frac{m^2\pi^2}{8a^2}(A^2-A_0^2). \tag{28}$$

Dividing $\overline{u}$ by the plate length a, the average stress-average strain relationship is derived as follows:

$$\varepsilon=-\frac{1}{E}\sigma-\frac{m^2\pi^2}{8a^2}(A^2-A_0^2). \tag{29}$$

Plastic Range

Based on rigid-plastic mechanism analysis, the average stress-average strain relationship is derived as:

$$\varepsilon=-\frac{1}{E}\sigma-\frac{2m^2}{a^2}(A^2-A_0^2) \quad \text{for} \quad \alpha \le 1.0, \tag{30}$$

$$\varepsilon=-\frac{1}{E}\sigma-\frac{2m^2}{ab}(A^2-A_0^2) \quad \text{for} \quad \alpha > 1.0. \tag{31}$$

Procedure to Obtain the Average Stress-Average Strain Curve

The average stress-deflection relationship changes from that explained by Equation 21 to that explained by Equation 23 or 24 at the ultimate strength. Until ultimate strength is attained, the average stress-average strain relationship is expressed by Equation 29. After the ultimate strength, the relationships of Equation 30 or 31 are followed. The ultimate strength (σ_{ULTt}) of the plate is accurately estimated by the author's formulas [7] as follows:

$$\sigma_{ULT}/\sigma_Y=\begin{cases}1.0 & \text{for} \quad \beta \le 1.73\\ 0.1+1.571/\beta & \text{for} \quad \beta > 1.73\end{cases}. \tag{32}$$

The procedure is shown schematically in Figure 8. A computer program was written in the Fortran 77 language, in order to implement the explained procedure.

Accuracy of the Method for Plates

The accuracy of the average stress-average strain relationships obtained by the analytical formulas and expressions derived above, are verified against those obtained applying FEA (Figure 9). The plate model applied in FEA and its meshing and boundary conditions have been shown in Figure 10. In order to

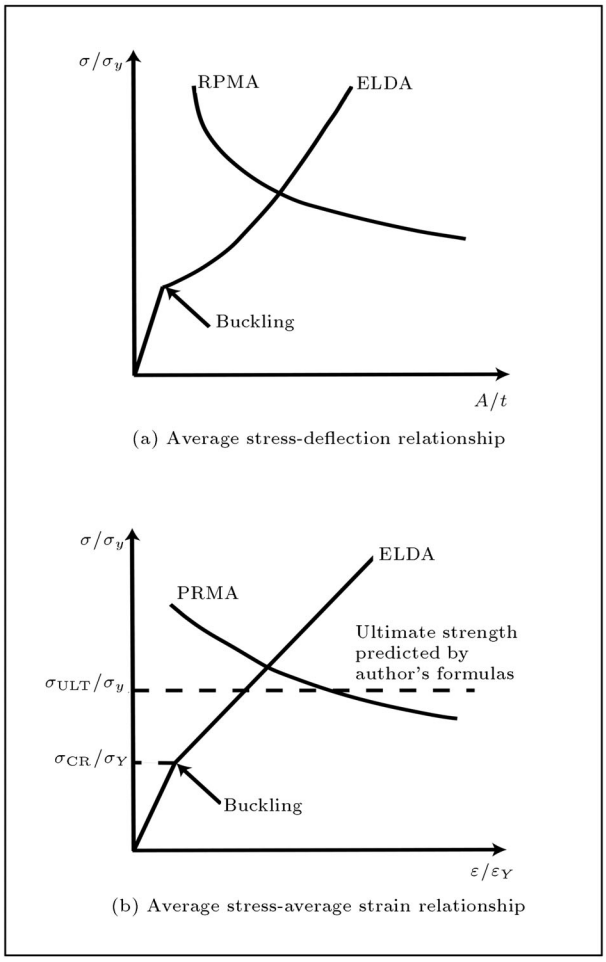

Figure 8. Schematic representation of the average stress-deflection and average stress-average strain relationships of the plate.

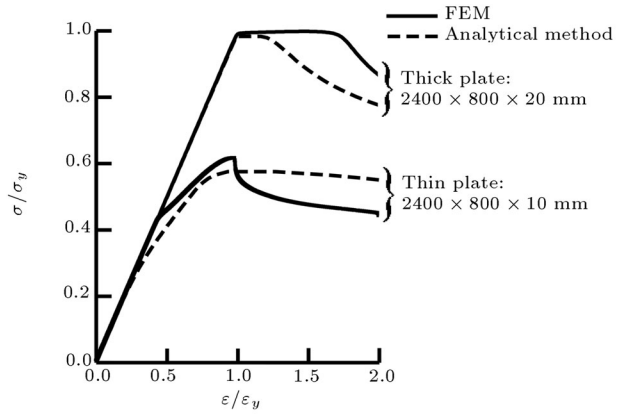

Figure 9. Comparison between simulated average stress-average strain relationships with FEA results (plates).

perform elastoplastic analysis of plates, the ULSAS code has been used. The ULSAS is a house made code developed in Hiroshima University [8] to model the collapse behavior of structures, considering the influence

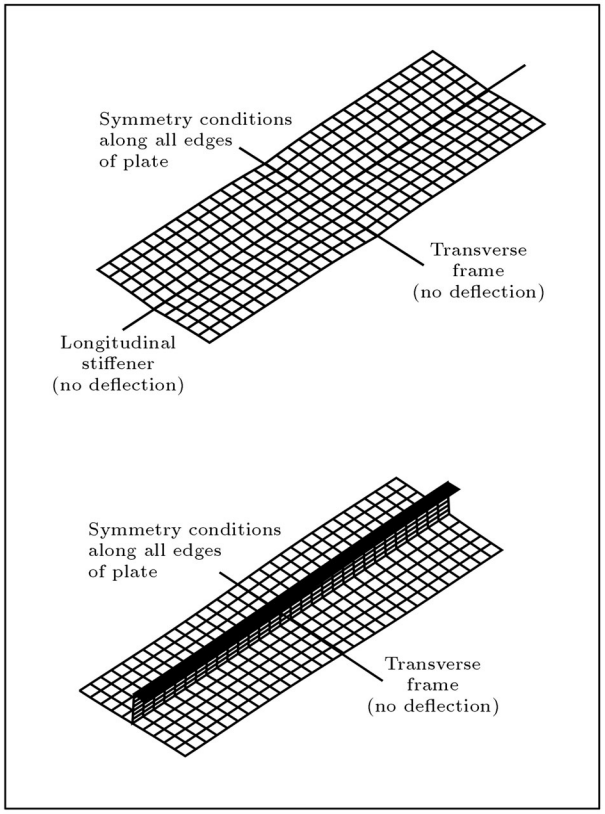

Figure 10. Plate and stiffened plate models applied in FEA, meshing and boundary conditions.

of material and geometrical nonlinearities induced by yielding and large deflection. An isoparametric shell element with four nodal points was used. They are degenerated elements with a linear displacement field and a reduced integration. Axial compression was simulated by an imposed displacement in a longitudinal direction, applied in small enough increments to ensure that the analysis would closely follow the model load-response curve. The same elastic-perfectly plastic behavior for material was assumed in the ULSAS FE code. As can be seen from the results, good correlations are observed among them.

AVERAGE STRESS-AVERAGE STRAIN RELATIONSHIP OF STIFFENED PLATES

Assumed Deflection Mode

The initial deflection mode of the stiffener element (stiffened plate) is assumed to be in the following mode [9]:

$$w_0 = \delta_0 \sin \frac{\pi x}{a}. \tag{33}$$

The total deflection under compressive axial load is expressed as the sum of the elastic and plastic components as below [10]:

$$w = w^e + w^p. \tag{34}$$

The elastic component is in the same mode as the initial deflection mode:

$$w^e = \delta_m \sin \frac{\pi x}{a}. \tag{35}$$

Based on [9], the coefficient of the elastic component is:

$$\delta_m = \delta_0/(1 - P/P_{cr}), \tag{36}$$

where P is the axial compressive load and P_{cr} is the elastic buckling load. The plastic component is [10]:

$$w^p = \begin{cases} 2cx/a & 0 \le x < 0.5(a - a^p) \\ c\left[-\frac{2x^2}{aa^p} + \frac{2x}{a^p} + 1 - 0.5\left(\frac{a}{a^p} + \frac{a^p}{a}\right)\right] & \\ & 0.5(a-a^p) \le x < 0.5a \end{cases}. \tag{37}$$

From the assumed deflection modes, the curvature, κ, and its components at the mid-span point, are derived as follows:

$$\kappa = \kappa^e + \kappa^p,$$

$$\kappa^e = (\pi/a)^2(\delta_m - \delta_0),$$

$$\kappa^p = 4c/aa^p. \tag{38}$$

Deflection and curvature components in a single span are shown in Figure 11. a^p is the length of yielded zone, which is evaluated according to the method expressed in [10].

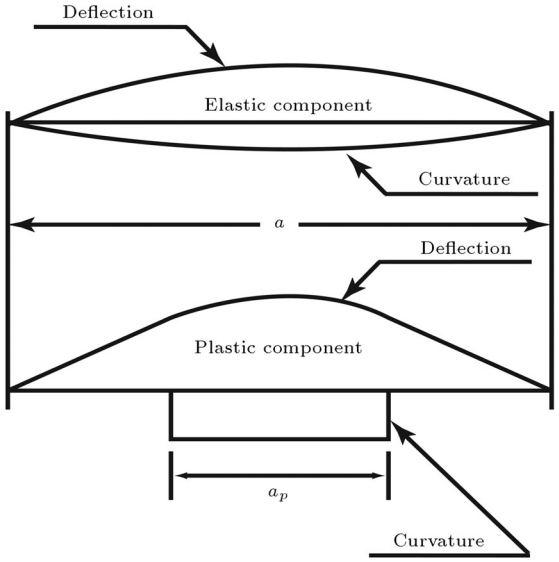

Figure 11. Elastic and plastic components of deflection and curvature.

Axial Force and Bending Moment in Cross-Section

The stress and strain distributions at cross-sections 1 and 2 take one of the patterns shown in Figure 12. In the plate part, the stress-strain relationship developed in the previous section is used. Axial forces and bending moments at each cross-section are evaluated by integrating stresses in Figure 12.

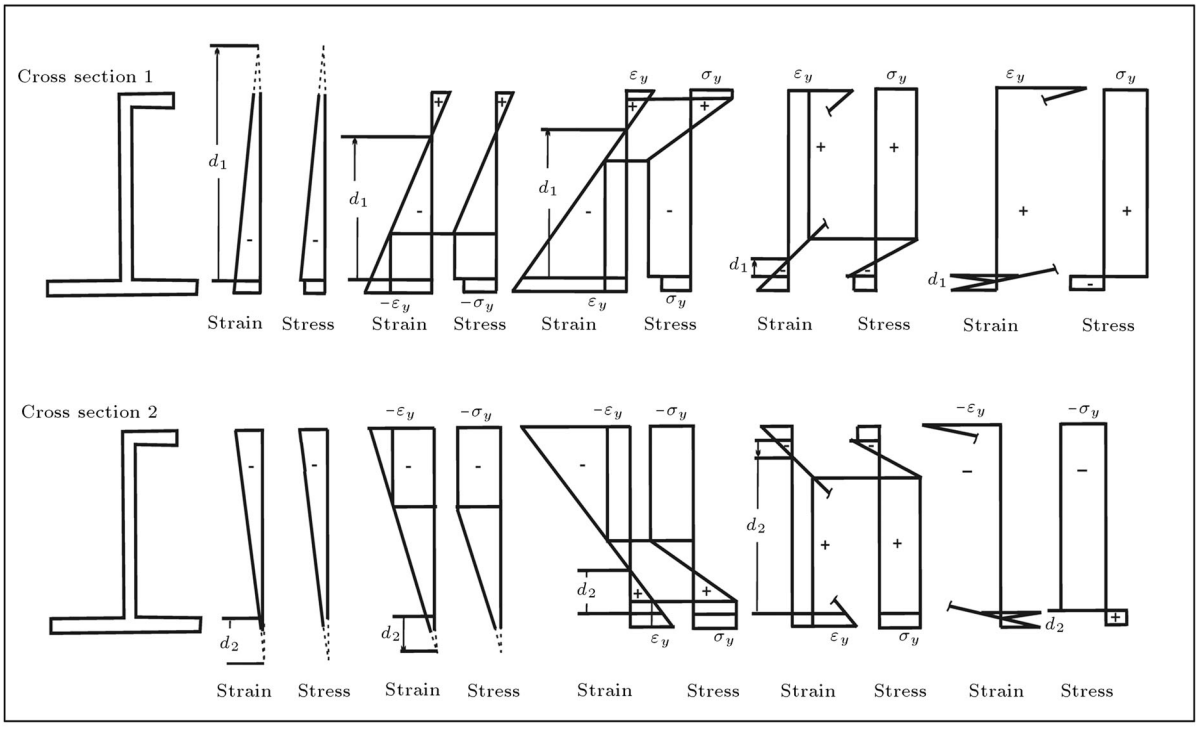

Figure 12. Possible stress and strain distributions at the cross-sections 1 and 2 [10].

Equilibrium Conditions

Neglecting the reaction forces at supporting points, the equilibrium conditions are:

$$P_1 = P_2, \quad M_2 + M_1 = W(P_1 + P_2)/2, \tag{39}$$

where P_1, P_2, M_1 and M_2 are shown in Figure 13. Since the strains in plating in sections 1 and 2 are different from each other, the point of zero-bending moment moves along the span from the original supporting point as the axial compressive load increases. Denoting the distances between zero-bending moment point and sections 1 and 2 by a_1 and a_2, one has:

$$P_{cr1} = \pi^2 EI_1/a_1^2, \quad P_{cr2} = \pi^2 EI_2/a_2^2, \tag{40}$$

where EI_1 and EI_2 are bending rigidities at cross-sections 1 and 2. a_1 and a_2 are determined from the following conditions:

$$\begin{cases} a_1 + a_2 = 2a \\ P_{cr1} = P_{cr2} \end{cases}, \tag{41}$$

so:

$$a_1 = 2a/(1+\beta), \quad a_2 = 2a\beta/(1+\beta), \tag{42}$$

where $\beta = \sqrt{(EI_2)/(EI_1)}$. When both spans are elastic, the ratio of curvatures at cross-sections 1 and 2 is:

$$\kappa_2/\kappa_1 = 1/\beta. \tag{43}$$

Relationship Between Average Stress and Average Strain

After satisfying equilibrium conditions, the axial compressive strain is evaluated as [7]:

$$\varepsilon = \varepsilon^0 + \frac{1}{2a}\sum_{i=1}^{2}\int_0^{a_i}\left[\varepsilon_i^k + 0.5\left(\frac{dw_i}{dx}\right)^2\right]dx, \tag{44}$$

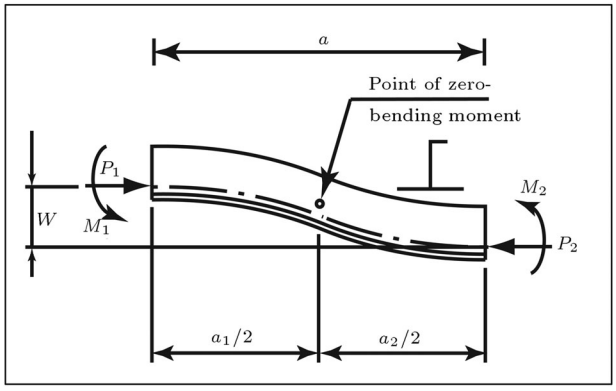

Figure 13. Forces and bending moments acting at both ends of the double-span model.

where $\varepsilon^0 = P/EF$ and $\varepsilon_i^k = \kappa_i(d_i - e) - \varepsilon^0$. F, e and d_i represent the sectional area, the location of original neutral axis and the current location of zero-stress point, respectively. The subscript, i, indicates the corresponding span or cross-section.

Procedure to Obtain the Average Stress-Average Strain Curve

The average stress-average strain relationship of the stiffened plate element is derived according to the flow chart shown in Figure 14.

Accuracy of the Method for Stiffened Plates

The accuracy of the average stress-average strain relationships, obtained by using the explained method, are verified against those obtained applying FEA (Figure 15). The plates are of dimensions 2400 × 800 mm. Different plate thicknesses and different stiffener cross-sections are considered. The same code (ULSAS), shell

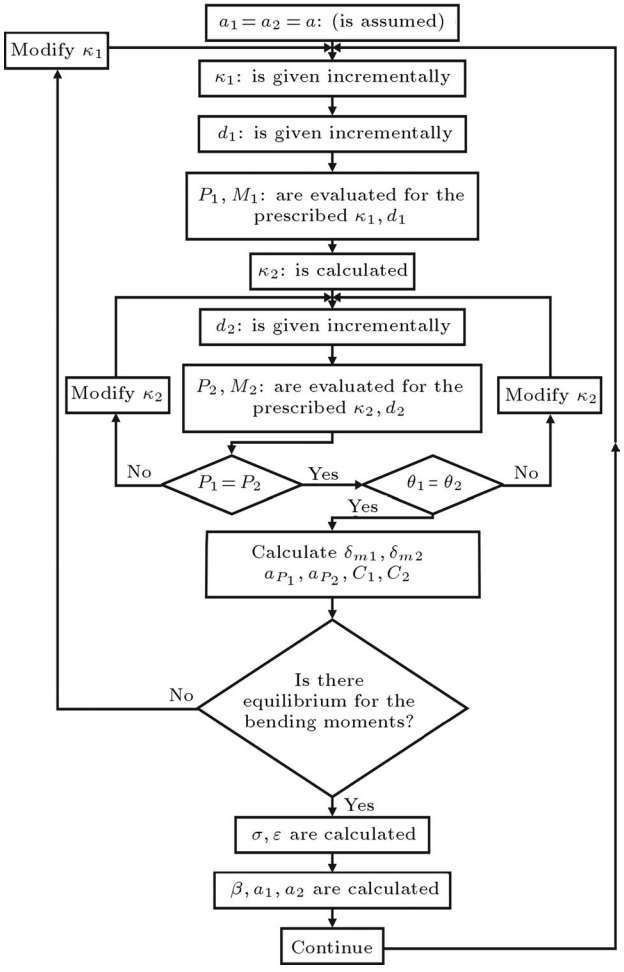

Figure 14. Flow chart of the method for derivation of the average stress-average strain relationship of the stiffened plate [7].

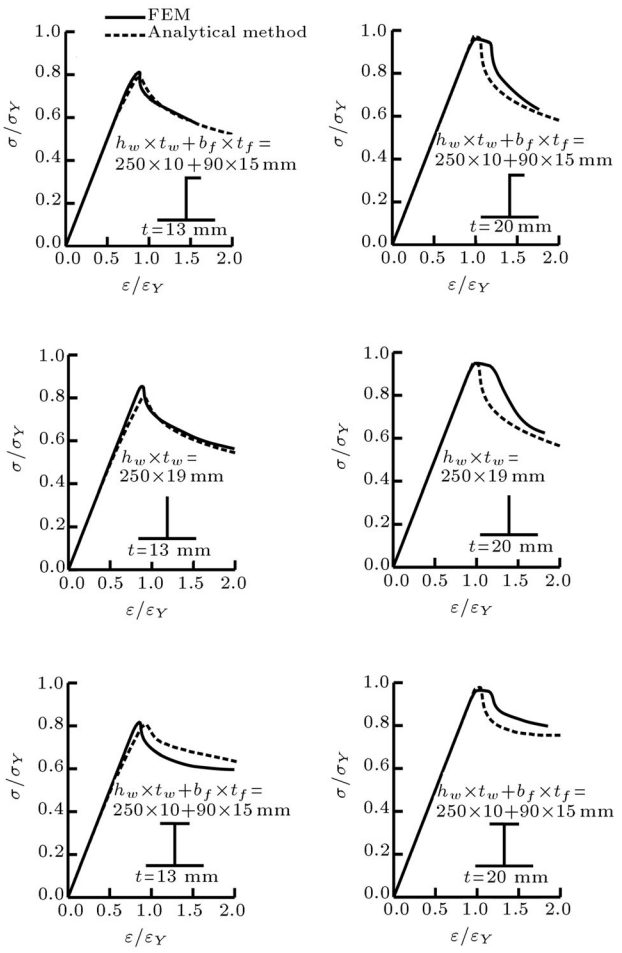

Figure 15. Comparison between simulated average stress-average strain relationships with FEA results (stiffened plates).

elements and simulation method were applied in the FE model of stiffened plates. A sample of an FE model of stiffened plate has been shown in Figure 10. Relatively good correlations are observed among the results.

CONCLUSIONS

A simple method for simulation of the average stress-average strain relationships of plates and stiffened plates, under the action of longitudinal axial compression, is developed. The features of the method are:

1. The results of elastic large deflection analysis and rigid-plastic mechanism analysis are combined together in the derivation of the average stress-average strain relationship of the plates;
2. Applying a double span model of the stiffened plate and imposing equilibrium conditions of forces and moments at the end sections of the model, the average stress-average strain relationship of the stiffened plate model is derived;
3. In both derivations, the influences of buckling and plastic deformations are considered;
4. The results show that the explained method is simple and relatively accurate and can be applied effectively in the ultimate strength evaluation of ship hull girders.

REFERENCES

1. Smith, C.S. "Influence of local compressive failure on ultimate longitudinal strength of a ship's hull", *PRADS*, Tokyo, Japan (1977).
2. Smith, C.S. "Structural redundancy and damage tolerance in relation to ultimate ship hull strength", *Int. Symp. on the Role of Design, Inspection and Redundancy in Marine Structural Reliability*, Williamsburg (1983).
3. Ueda, Y. and Yao, T. "The influence of complex initial deflection on the behavior and ultimate strength of rectangular plates in compression", *J. of Const. Steel Research*, **5**, pp 265-302 (1985).
4. Yao, T., Nikolov, P.I. and Miyagawa, Y. "Influence of welding imperfections on stiffness of rectangular plates under thrust", *Proc. of IUTAM Sump. on Mechanical Effects of Welding*, K. Karlsson, L.E. Lindgren, and M. Jonsson, Eds., Springer-Verlag, pp 261-268 (1992).
5. Varghese, B. " Buckling/plastic collapse strength of plates and stiffened plates under combined loads", Dr. Eng. Thesis, Hiroshima University, Japan (Jan. 1998).
6. Okada, H., Oshima, K. and Fukumoto, Y. "Compressive strength of long rectangular plates under hydrostatic pressure", *J. of Soc. Naval Arch. of Japan*, **146**, pp 270-280 (in Japanese) (1979).
7. Khedmati, M.R. "Ultimate strength of ship structural members and systems considering local pressure effects", Dr. Eng. Dissertation, Grad. School of Eng., Hiroshima University, Japan (2000).
8. Yao, T., *ULSAS: FEM Code for Non-Linear Analysis of Structures*, Hiroshima University, Japan (2000).
9. Timoshenko, S.P. and Gere, J.M., *Theory of Elastic Stability*, McGraw-Hill (1961).
10. Bai, Y. "Marine structural design", Lecture Notes, Stavanger University College, Norway (2000).